IOP Publishing | Astro Ltd
Laser Physics Letters
Laser Phys. Lett. **15** (2018) 116201 (6pp)
https://doi.org/10.1088/1612-202X/aadc5a

Letter

Low-frequency fluctuations of a mid-infrared quantum cascade laser operating at cryogenic temperatures

Olivier Spitz[1,2,3,6], **Jiagui Wu**[3,4,6], **Mathieu Carras**[2], **Chee-Wei Wong**[3] and **Frédéric Grillot**[1,3,5]

[1] LTCI Télécom ParisTech, Université Paris-Saclay, 46 rue Barrault, Paris, 75013, France
[2] mirSense, Centre d'intégration NanoInnov, 8 avenue de la Vauve, Palaiseau, 91120, France
[3] Fang Lu Mesoscopic Optics and Quantum Electronics Laboratory, University of California Los Angeles, Los Angeles, CA 90095, United States of America
[4] College of Electronic and Information Engineering, Southwest University, Chongqing 400715, People's Republic of China
[5] Center for High Technology Materials, University of New-Mexico, 1313 Goddard SE, Albuquerque, NM 87106, United States of America

E-mail: olivier.spitz@telecom-paristech.fr

Received 13 August 2018
Accepted for publication 20 August 2018
Published 14 September 2018

Abstract

This work demonstrates that mid-infrared quantum cascade lasers operating under external optical feedback can output a chaotic dynamics through low-frequency fluctuations close to 77 K. Results also show that the birth of chaotic dynamics is not limited to near-threshold pumping levels. In addition, when the semiconductor material is cooled down from room temperature to 77 K, it is found that laser destabilization takes place at a lower feedback ratio, proving that quantum cascade lasers are sensitive to temperature, likely due to changes in the upper state lifetime. These investigations are meaningful for the chaotic operation of quantum cascade lasers in secure atmospheric transmission lines and optical countermeasure systems.

Keywords: quantum cascade laser, mid-infrared, optical feedback, non-linear dynamics

(Some figures may appear in colour only in the online journal)

1. Introduction

Quantum cascade lasers (QCLs), conceived for the first time in the early 1970s [1] and demonstrated in 1994 [2], are unipolar semiconductor laser sources based on intersubband transitions which have proven to be powerful, tunable and versatile mid-infrared light sources operating at room temperature [3]. The wide range of achievable wavelengths from the mid-infrared to the terahertz domain paves the way for multiple applications [4] such as optical countermeasures for defense purposes, particle detection below one per million, jamming-resistant free-space communications and LIDAR remote sensing [5], all demanding stable single-mode operation with a narrow linewidth, high output power and high modulation bandwidth. External optical feedback consisting of re-injecting part of the light of a semiconductor laser in order to modify its emission properties has been studied for a wide range of purposes [6]. It has a strong influence on the QCL dynamics and several feedback regimes have been analogously identified with interband diode lasers [7], including noise reduction [8] or mode selection in widely tunable sources [9]. However, in contrast to interband lasers where the carrier-to-photon lifetime is around 10^3, QCLs exhibit a sub-picosecond intersubband carrier dynamics, leading to a very small carrier-to-photon lifetime ratio

[6] The authors contributed equally to this work.

around 0.1 [10]. Recent work showed that mid-infrared QCLs under external optical feedback can experience a route to chaos when pumped close to the threshold [11]. The latter was first observed through a Hopf bifurcation to periodic dynamics at the external cavity frequency and then through low frequency fluctuations (LFF), which is a signature of deterministic chaos. The LFF can be described as a competition between modes which are located on a feedback ellipse. The trajectory wanders around an external cavity mode for a few revolutions and then hops to the next mode with a higher intensity, repeating it until it reaches the highest order mode where the collision with its antimode produces the drop off [6]. In addition, experiments proved that the route to chaos was not associated with the undamping of the relaxation oscillations, which strongly differs from what is commonly observed in interband semiconductor lasers [6]. This work goes a step further by investigating the impact of temperature on the nonlinear dynamics properties of a mid-infrared QCL operating under external optical feedback. In particular, it is shown that the LFF regime remains highly sustained in liquid nitrogen (77 K) and that its occurrence is not limited to near-threshold operation. Overall, when the QCL is cooled down from room temperature (290 K) to 77 K, experiments reveal that laser destabilization appears at a lower feedback ratio owing to a 100% increase of the upper state lifetime between 290 K and 77 K, which is also confirmed by a numerical analysis. These novel insights are meaningful for understanding and controlling the intersubband dynamics as well as for developing secure atmospheric transmission lines and optical countermeasure systems.

2. Methods

The QCL from mirSense under study is 2 mm long and 14 μm wide, with emission at a wavelength of 5.6 μm. The device consists of a distributed feedback laser working in single mode operation, achieved via a metal grating cladding at the top of the laser ridge. One of the facets of the laser is highly reflective and the other one is cleaved to have a 70% transmission coefficient, allowing the light to be emitted from the QCL but also the back-reflected wave to couple inside the laser cavity. The laser ridge is made of two InP cladding layers surrounding the 1.5 μm active region, which consists of 30 periods of strained AlInAs/GaInAs grown by molecular beam epitaxy, inspired by a design from [12]. The laser die is epi-side down mounted using AuSn to an AlN submount to ensure good thermal dissipation, as shown in figure 1. Indeed, the QCL is pumped with a quasi-continuous wave and this induces strong heating of the whole structure. This QCL exhibits a threshold current I_{th} of 590 mA when pumped at 290 K with a 300 ns pulse at a repetition rate of 100 kHz (i.e. a 3% duty cycle). At 77 K, the threshold current is 331 mA and the current leading to the maximum emitted power is 950 mA. The QCL emits single-mode at 1775 cm^{-1} (corresponding to an optical wavelength of 5.63 μm), as shown in figure 2.

Figure 3 shows that the external optical feedback set up is composed of two parts. On the one hand, there is a back-reflection path with a polarizer designed for mid-infrared light

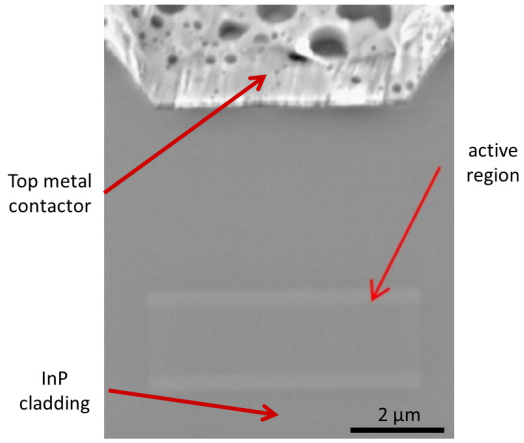

Figure 1. Scanning electron micrograph of a buried heterostructure quantum cascade laser.

and a gold-plated mirror placed on an accurately moving cart. This mirror defines the external cavity length which is one of the main parameters of external optical feedback. The polarizer is a key optical device for varying the amount of optical feedback knowing that the QCL wave is indeed TM polarized. This defines the feedback ratio f, standing for the ratio between the back-reflected power that couples inside the laser cavity and the total power emitted by the laser. In what follows, the optical feedback f is controlled by rotating the polarizer. In the detection path, we use a high bandwidth mid-infrared detector (Vigo PEM mercury–cadmium–telluride; MCT) operating at room temperature. The signal retrieved from the MCT detector is amplified with a low noise amplifier (Mini-Circuits ZFLN-1000) with a bandwidth of 1000 MHz in order to overcome the background noise. This is subsequently analyzed with a real time 500 MHz oscilloscope. For an external cavity length between 30 and 60 cm, the related frequency at which the destabilization takes place in the laser is between 500 and 250 MHz within the oscilloscope bandwidth. Indeed, no relaxation oscillations appear in a QCL, in contrast to what is usually found in diode lasers. A 60/40 mid-infrared beam splitter then splits the focused laser beam into both paths. Focusing is achieved with a lens in front of the laser. Two different setups are implemented based on the measurement temperature. When the laser is studied at room temperature, the QCL package is horizontally clamped over an indium foil and a copper mount with a Peltier module for temperature control. In that configuration, the wave hitting the beam splitter is P-polarized and the transmission of the beam splitter at this wavelength is about 60%. Low temperature measurements down to 77 K are implemented in a cryostat. The QCL is vertically clamped over a copper mount, the latter being placed inside a vacuum chamber in order to insulate from the outside. A heater and a temperature controller inside the vacuum chamber allow better control of this key parameter. The cryostat has an output covered with a ZnSe window made for mid-infrared light and a focusing lens is placed between this window and the beam splitter. The wave hitting the beam splitter is S-polarized and the maximum achievable transmission is 35% because the QCL is vertically inserted inside the vacuum chamber. In order to minimize the environmental perturbations, such as acoustic

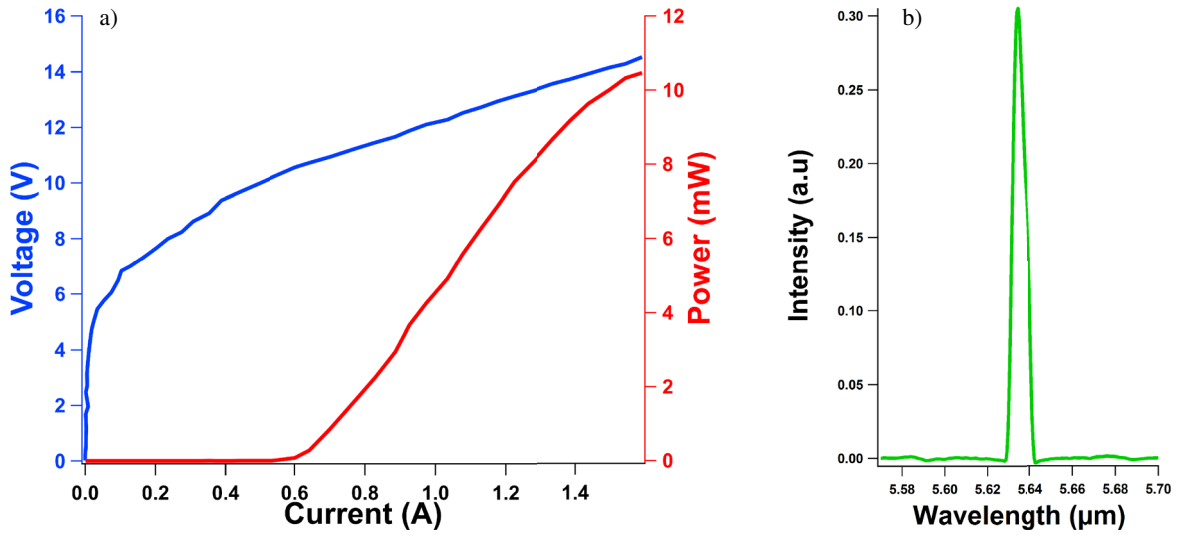

Figure 2. LIV and spectral (inset) characteristics of the free-running QCL operating at 290 K and under a pulsed wave with a 3% duty cycle.

and mechanical noises, the laser is mounted on a suspended optic table. Consequently, the feedback mirror remains immobile and the observed pattern cannot be related to self-mixing effects. Furthermore, the applied feedback ratios are well above the ones required for self-mixing interferometry [13].

3. Results

Initial experiments showed that the LFF chaotic regime was observed when driving the QCL very close to the threshold at $I = 1.005 \times I_{th}$ [11] whereas in our case, the laser operates at a high bias current, i.e. $I = 2.2 \times I_{th}$ at 290 K and at 77 K. In what follows, the laser is biased with a quasi-continuous source which emits a 2 μs pulse and the external cavity length is set to 35 cm which leads to an external cavity frequency of 430 MHz. Figure 4 displays the temporal waveforms recorded at 290 K (a) with $f = 0.246$ and at 77 K (b) with $f = 0.089$. These measurements show that the LFF dynamics is still highly sustained at 77 K and, in addition, the operating feedback can be much smaller than that used at room temperature. In both cases, the chaotic pattern is composed of slow oscillations modulated by faster ones. The fast oscillations occur at a frequency close to the external cavity roundtrip frequency, which is 320 MHz, as illustrated in the signal FFT (inset of figure 4). The 320 MHz peak is in the same order-of-magnitude as our expectations, though slightly lower than our theoretical estimates. The slight deviation is attributed to the transient regime that still appears in the pulse due to the internal heating of the structure. The slow oscillation is about 20 MHz and corresponds to the contribution of the low-frequency chaotic dynamics as already reported elsewhere [6]. However, as compared to the LFF pattern reported in [11], our measurements illustrate another LFF regime taking place at higher injected currents, in a similar way to interband diode lasers [14]. As the QCL is pumped well above the threshold and because the bias current is fixed during the whole experiment, the retrieved LFF pattern is purely delay-induced and

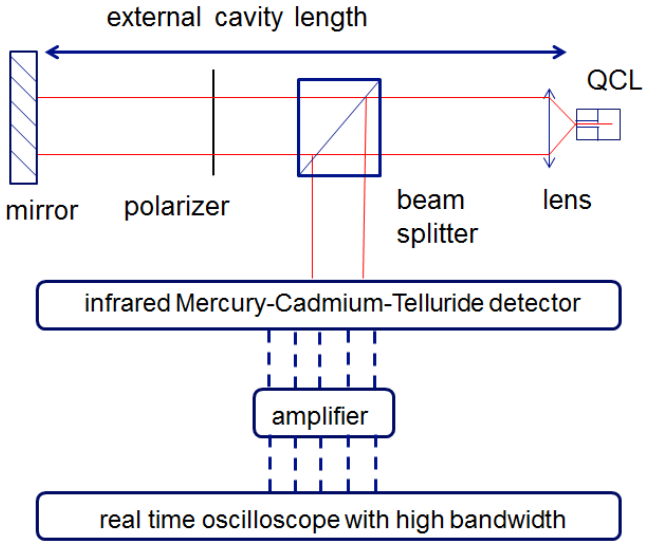

Figure 3. Experimental setup with the feedback path allowing control of the back-reflected light and the detection path.

is not connected with, or is not supported by, a possible noise current source dependence.

Figure 5 exhibits the whole evolution of the temporal waveforms of the QCL for different amounts of external optical feedback f at 77 K. For each trace, the transient regime lasts between 0.8 and 1.2 μs. It can be clearly seen for figures 5(f) and (g) until approximately 1.2 μs. Under free-running operation ($f = 0$), the QCL operates in a steady-state, and hence the time trace is unchanged. Let us note that the latter is not completely flat because the amplifier used for the experiments had a low-frequency cutoff below 100 kHz and therefore part of the square signal harmonics are lost. When the feedback is slightly increased to $f = 0.0003$, oscillations start to appear and hence the QCL is likely operating in a limit cycle with an oscillation frequency slightly smaller than the external cavity, as aforementioned. At $f = 0.0003$ and $f = 0.0008$, the traces do not exhibit an LFF pattern. The latter is observed for

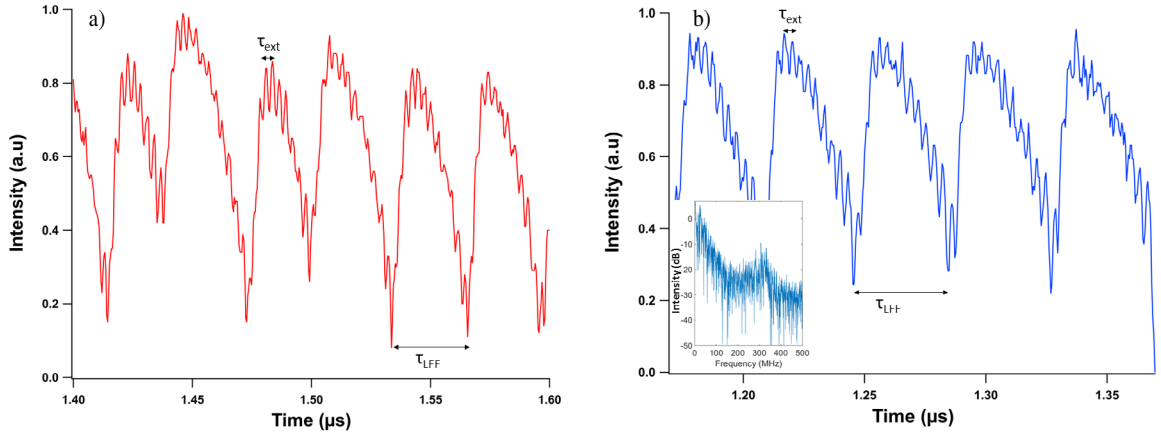

Figure 4. Close-up of the LFF dynamics at 290 K for $f = 0.246$ (a) and at 77 K for $f = 0.089$ (b) with the fast Fourier transform of the time trace in the inset.

feedback ratios above 0.0046. At $f = 0.0298$, $f = 0.0393$ and $f = 0.089$, an increase of the back-reflected light gives rise to a pattern composed of pure LFF with an intensity modulation, as described in figure 5(g). At the maximum reachable feedback, the time trace at 77 K also exhibits another stage with lower frequencies, as shown in figure 5(i). This step was never reached at 290 K, even when the feedback ratio was higher than in our cryogenic measurements here. The coexistence of LFF with more complex dynamics is a good precursor for generating chaos with a higher dimensionality. To confirm the chaotic behavior, we calculated the Lyapunov exponents (LEs) from the time traces, which describe the divergence rate of nearby attractor trajectories and are widely used criterion in defining chaos [15, 16]. Positive LEs indicate the ultra-sensitivity to initial conditions of a chaotic state [15–20]. The phase portraits (figure 6(a) for 290 K, figure 6(c) for 77 K) of the temporal waveforms are plotted and show the rich attractor structure. The four largest Lyapunov exponents (LLEs) are also given in figures 6(b) and (d), for 290 K and 77 K respectively. First, in figure 6(b), the calculated LLEs converge to values $\lambda_1 = 0.485\ \mu s^{-1}$, $\lambda_2 = 0.284\ \mu s^{-1}$, $\lambda_3 = -0.021\ \mu s^{-1}$ and $\lambda_4 = -0.656\ \mu s^{-1}$ at the 290 K condition. The two maximum LEs are positive, illustrating a fast divergence rate between adjacent orbits and indicating that the system is in a chaotic state. The third LE has a value of nearly zero, which is related to the periodic part in the chaotic temporal evolution of QCL. The LEs of the QCL operating at cryogenic temperatures (77 K) are also calculated. The LE curves converge to the values $\lambda_1 = 0.444\ \mu s^{-1}$, $\lambda_2 = 0.238\ \mu s^{-1}$, $\lambda_3 = -0.002\ \mu s^{-1}$ and $\lambda_4 = -0.582\ \mu s^{-1}$, respectively. The positive LE values clearly illustrate that the QCL system is under a chaotic state and even an upper chaos state since there are two positive LEs [15, 16]. Different LFF regimes were originally pointed out in interband diode lasers [14] while a recent paper has even analyzed the dynamical transitions between them, showing the birth of well-defined dropouts near the threshold, followed by faster and irregular fluctuations at higher pumps [21]. Although a route to chaos involving periodic oscillations at the external cavity frequency followed by deterministic LFF is also observed at 77 K in agreement with [11], this work shows that decreasing the

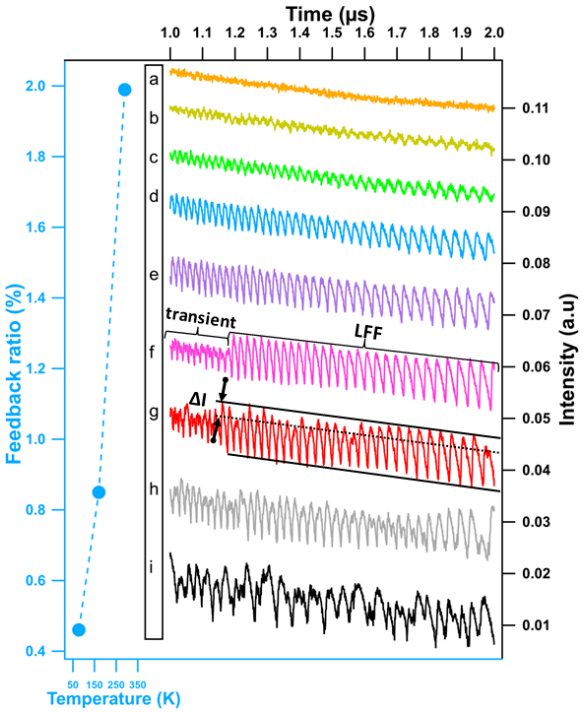

Figure 5. Experimental time traces of the QCL under optical feedback at 77 K. The polarizer allows us to achieve a value of feedback ratio f between 0 and 0.089. (a) $f = 0$. (b) $f = 0.0003$. (c) $f = 0.0008$. (d) $f = 0.0046$. (e) $f = 0.0141$. (f) $f = 0.0213$. (g) $f = 0.0298$. (h) $f = 0.0393$. (i) $f = 0.089$. The left part shows the required critical feedback leading to LFF emergence for three temperatures: 290 K, 170 K and 77 K; the dashed blue line is for the visual guidance of the reader.

temperature makes the QCL more sensitive to the optical feedback with LFF dynamics taking place over a wide range of feedback levels. Indeed, at 290 K, a feedback ratio as high as 0.0199 is required to observe the birth of the LFF dynamics while it does not exceed 0.0046 here at 77 K (0.0085 at 170 K as shown in figure 5 left axis). Such a difference can be attributed to the increase of the carrier-to-photon lifetime ratio. At room temperature, the latter is typically of the order of 0.1 in a QCL whereas it is four orders of magnitude larger in interband lasers [22].

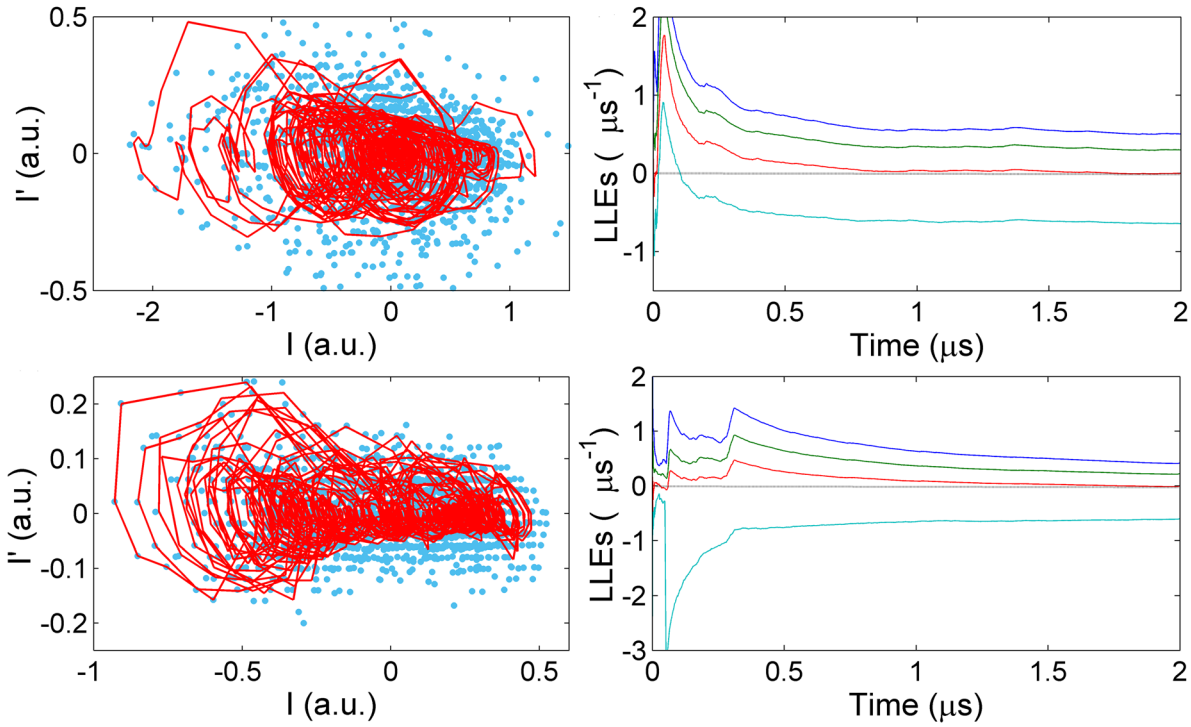

Figure 6. System dynamics analysis through Lyapunov exponents (LEs). The upper row is the combination for the 290 K case. The lower row is the combination for the 77 K case. Each combination includes the phase portrait ((a) and (c)) of the temporal waveform and the calculated spectrum of the Lyapunov exponents ((b) and (d)). As the time evolves, curves in each panel converge to the values of such exponents. Only the largest four LEs are plotted in each diagram. For the calculated spectra, the curves converge to values (b) $\lambda_1 = 0.485\ \mu s^{-1}$, $\lambda_2 = 0.284\ \mu s^{-1}$, $\lambda_3 = -0.021\ \mu s^{-1}$ and $\lambda_4 = -0.656\ \mu s^{-1}$ under 290 K, and values (d) $\lambda_1 = 0.444\ \mu s^{-1}$, $\lambda_2 = 0.238\ \mu s^{-1}$, $\lambda_3 = -0.002\ \mu s^{-1}$ and $\lambda_4 = -0.582\ \mu s^{-1}$ under 77 K. The blue dots in the left diagrams are the retrieved values of the derivative of the laser's intensity I' as a function of the laser's intensity I and the red curve represents the phase diagram after noise filtering.

The carrier lifetime can be approximated via the upper-state lifetime τ_c, [23] defined as follows :

$$\frac{1}{\tau_c} \approx \frac{1}{\tau_{31}} + \frac{1}{\tau_{32}} \tag{1}$$

with τ_{32} the time constant related to the carrier scattering into the lower laser level and τ_{31} the one into the bottom level with a time constant through longitudinal–optical phonon emissions (the energy levels are shown in the inset of figure 7). In this work, the upper-state lifetime is investigated with a custom heterostructure simulation software named METIS based on semi-classical Boltzmann equations with thermalized sub-bands [24]. Figure 7 shows the evolution of τ_c from 373 K down to 73 K with steps of 20 K. Other numerical studies using a density matrix transport model showed similar results for the carrier lifetime of mid-infrared QCLs [25]. For each temperature, the upper bound represents the value of τ_c just above the threshold and the lower bound represents the value of τ_c close to the current value leading to the maximum output power. Numerical simulations show that the mean upper state lifetime increases from 0.47 ps to 1.26 ps when cooling down the device which corresponds to a total variation of about 170%. The latter directly transforms into a larger carrier-to-photon lifetime ratio. Assuming the photon lifetime is slowly varying compared to the upper state lifetime between 290 K and 77 K, [26] the carrier-to-photon lifetime is thus expected

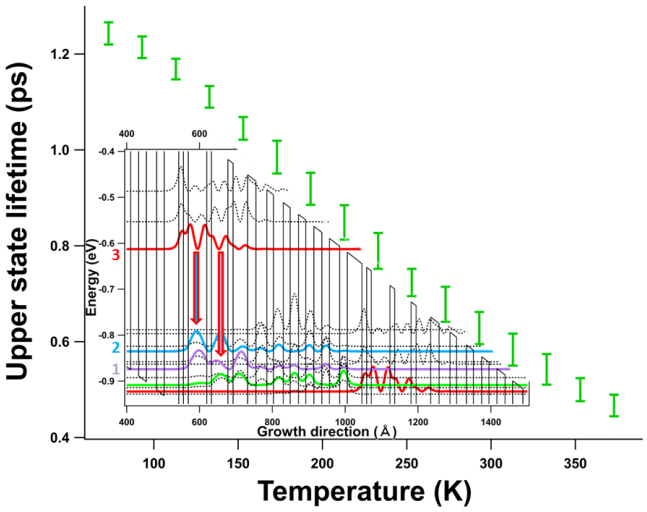

Figure 7. Simulation of the upper state lifetime evolution with temperature for the QCL under study. The inset shows the wavefunctions and energy levels for this QCL at 290 K.

to increase from 0.13 to 0.26 on average. This largely explains the increased sensitivity to the external optical feedback of the QCL in this study, as underlined in the Lang and Kobayashi model for semiconductor lasers under external optical feedback [27] in which the carrier-to-photon lifetime ratio plays a predominant role. However, in comparison with diode lasers in which the threshold leading to instabilities usually decreases

at higher temperatures due to a reduced output power and a larger linewidth enhancement factor [28], this work shows that the QCL becomes more sensitive to optical feedback at low temperatures, despite a larger output power. As a consequence, other parameters, such as the linewidth enhancement factor and the damping rate which were not studied in that experiment, may also vary with temperature and further influence the QCL sensitivity to optical feedback.

4. Conclusion

To summarize, we qualitatively retrieve experimental evidence showing the main feedback regimes and a bifurcation process from steady state to LFF dynamics through a limit cycle, the deterministic chaotic behavior being confirmed by a Lyapunov exponent analysis. We show that the LFF regime is stronger at 77 K owing to a 100% increase of the upper state lifetime between 290 K and 77 K. As a result, the laser destabilization takes place at a lower feedback ratio through an increase of the carrier-to-photon lifetime ratio, which is an important feature for understanding the underlying physics of QCLs. This work paves the way towards the development of possible secure atmospheric transmission lines and unpredictable optical countermeasures operating in the mid-infrared wavelengths.

Acknowledgments

This work is supported by the French Defense Agency (DGA), the French ANR program under grant ANR-17-ASMA-0006, the Office of Naval Research (N00014-16-1-2094) and the National Science Foundation (DMR-1611598). The authors acknowledge Dr Virginie Trinité for helping with METIS, Zhangji Zhao for assistance in the cryogenic measurements, Prof. Benjamin S Williams and Dr Sudeep Khanal for fruitful discussions.

References

[1] Kazarinov R F and Suris R A 1971 *Sov. Phys. Semicond.* **5** 707–9
[2] Faist J, Capasso F, Sivco D L, Sirtori C, Hutchinson A L and Cho A Y 1994 *Science* **264** 553–6
[3] Yao Y, Hoffman A J and Gmachl C F 2012 *Nat. Photonics* **6** 432
[4] Capasso F 2010 *Opt. Eng.* **49** 111102
[5] Lin F Y and Liu J M 2004 *IEEE J. Sel. Top. Quantum Electron.* **10** 991–7
[6] Kane D M and Shore K A 2005 *Unlocking Dynamical Diversity: Optical Feedback Effects on Semiconductor Lasers* (New York: Wiley)
[7] Jumpertz L, Carras M, Schires K and Grillot F 2014 *Appl. Phys. Lett.* **105** 131112
[8] Ravaro M, Barbieri S, Santarelli G, Jagtap V, Manquest C, Sirtori C, Khanna S and Linfield E 2012 *Opt. Express* **20** 25654–61
[9] Hugi A, Maulini R and Faist J 2010 *Semicond. Sci. Technol.* **25** 083001
[10] Petitjean Y, Destic F, Mollier J C and Sirtori C 2011 *IEEE J. Sel. Top. Quantum Electron.* **17** 22–9
[11] Jumpertz L, Schires K, Carras M, Sciamanna M and Grillot F 2016 *Light: Sci. Appl.* **5** e16088
[12] Evans A, Yu J, David J, Doris L, Mi K, Slivken S and Razeghi M 2004 *Appl. Phys. Lett.* **84** 314
[13] Cardilli M C, Dabbicco M, Mezzapesa F P and Scamarcio G 2016 *Appl. Phys. Lett.* **108** 031105
[14] Heil T, Fischer I and Elsäßer W 1998 *Phys. Rev.* A **58** R2672
[15] Sprott J C 2003 *Chaos and Time-Series Analysis* (Oxford: Oxford University Press)
[16] Ott E 2002 *Chaos in Dynamical Systems* (Cambridge: Cambridge University Press)
[17] Grassberger P and Procaccia I 1983 *Physica* D **9** 189–208
[18] Schuster H G and Just W 2006 *Deterministic Chaos: an Introduction* (New York: Wiley)
[19] Grassberger P and Procaccia I 1983 *Phys. Rev. Lett.* **50** 346
[20] Strogatz S H and Herbert D E 1996 *Med. Phys.-New York-Inst. Phys.* **23** 993–5
[21] Quintero-Quiroz C, Tiana-Alsina J, Romà J, Torrent M and Masoller C 2016 *Sci. Rep.* **6** 37510
[22] Jumpertz L 2017 *Nonlinear Photonics in Mid-Infrared Quantum Cascade Lasers* (Berlin: Springer)
[23] Gensty T and Elsäßer W 2005 *Opt. Commun.* **256** 171–83
[24] Trinité V, Ouerghemmi E, Guériaux V, Carras M, Nedelcu A, Costard E and Nagle J 2011 *Infrared Phys. Technol.* **54** 204–8
[25] Talukder M A and Menyuk C R 2011 *New J. Phys.* **13** 083027
[26] Liu Z, Gmachl C F, Cheng L, Choa F S, Towner F J, Wang X and Fan J 2008 *IEEE J. Quantum Electron.* **44** 485–92
[27] Lang R and Kobayashi K 1980 *IEEE J. Quantum Electron.* **16** 347–55
[28] Carroll O, O'Driscoll I, Hegarty S P, Huyet G, Houlihan J, Viktorov E A and Mandel P 2006 *Opt. Express* **14** 10831–7